Antiviral Research 96 (2012) 234–244

Contents lists available at SciVerse ScienceDirect

Antiviral Research

journal homepage: www.elsevier.com/locate/antiviral

A novel minicircle vector based system for inhibting the replication and gene expression of Enterovirus 71 and Coxsackievirus A16

Zhuo Yang, Guodong Li, Yingqiu Zhang, Xiaoman Liu, Po Tien *

CAS Key Laboratory of Pathogenic Microbiology and Immunology, Institute of Microbiology, Chinese Academy of Sciences, Beijing 100101, China

ARTICLE INFO

Article history:
Received 6 April 2012
Revised 1 August 2012
Accepted 3 August 2012
Available online 17 August 2012

Keywords:
Enterovirus 71
Coxsackievirus A16
Minicircle vector
RNA interference
Antiviral therapy

ABSTRACT

Enterovirus 71 (EV 71) and Coxsackievirus A16 (CA 16) are two major causative agents of hand, foot and mouth disease (HFMD). They have been associated with severe neurological and cardiological complications worldwide, and have caused significant mortalities during large-scale outbreaks in China. Currently, there are no effective treatments against EV 71 and CA 16 infections. We now describe the development of a novel minicircle vector based RNA interference (RNAi) system as a therapeutic approach to inhibiting EV 71 and CA 16 replication. Small interfering RNA (siRNA) molecules targeting the conserved regions of the $3C^{pro}$ and $3D^{pol}$ function gene of the EV 71 and CA 16 China strains were designed based on their nucleotide sequences available in GenBank. This RNAi system was found to effectively block the replication and gene expression of these viruses in rhabdomyosarcoma (RD) cells and virus-infected mice model. The inhibitory effects were confirmed by a corresponding decrease in viral RNA, viral protein, and progeny virus production. In addition, no significant adverse off-target silencing or cytotoxic effects were observed. These results demonstrated the potential and feasibility of this novel minicircle vector based RNAi system for antiviral therapy against EV 71 and CA 16 infection.

1. Introduction

Hand, foot and mouth disease (HFMD) is a common viral illness among infants and young children, with clinical characteristics of prodromal fever followed by pharyngitis, mouth ulcers and a rash on the hands and feet (Chan et al., 2003; Chen et al., 2007). Human enterovirus 71 (EV 71) and coxsackievirus A16 (CA 16) are the two major causative agents of HFMD. Both EV 71 and CVA16 belong to the genus *Enterovirus* in the family *Picornaviridae* (Racaniello, 2007). Like other members of the family, both viruses contain a genome of single-stranded, positive sense RNA with a single open reading frame (ORF) encoding a large polyprotein precursor, and flanked by the 5′- and 3′-untranslated regions (UTRs). In infected cells, this polyprotein is cleaved into four structural (Vp1–Vp4) and seven non-structural (2A–2C; 3A–3D) proteins via the virus-encoded 2A and 3C proteases. The RNA-dependent RNA polymerase 3D is responsible for viral RNA replication (Shinohara et al., 2001).

Clinically, infections with either of the two viruses manifesting as HFMD are indistinguishable. However, EV 71 can also result in severe neurological diseases such as aseptic meningitis and acute flaccid paralysis (AFP), and even death (Chan et al., 2003; Chen et al., 2007; Wong et al., 2008). Since the first reported in New Zealand in 1957 (Robinson et al., 1958), HFMD has continued to spread globally and is a continuing threat to global public health (Alexander et al., 1994; Bible et al., 2008; Gilbert et al., 1988; Ho et al., 1999; Ishimaru et al., 1980). Previously, CA 16 was less well studied than EV 71 because the HFMD it caused was considered to be mild and harmless due to its relatively benign symptoms. Recent studies showed that CA 16 infection can be associated with serious myocarditis and pericarditis. The infection may cause cardiac arrhythmias, acute heart failure and fatal shock (Wang et al., 2004; Wright et al., 1963). In the past few decades, the Asia–Pacific region has suffered from frequent and widespread outbreaks of EV 71 and CA 16 infections (Solomon et al., 2010). Studies of many samples from patients with HFMD revealed that both EV 71 and CA 16 have contributed to recent outbreaks in China (Zhang et al., 2010; Qiu, 2008). Human can also be co-infected by EV 71 and CA 16 and carry the two viruses simultaneously. This dual-infection may contribute to the recombination observed between EV 71 and CA 16 which was thought to be responsible for the emergence of the new EV 71 genotype D (Yip et al., 2010). During these outbreaks, many individuals with HFMD suffered serious complications that resulted in death. Such outbreaks have raised public concerns about the virulence of EV 71 and CA 16. Thus far, no prophylactic or therapeutic method is available to treat HFMD (Zhang and Lu, 2010). These urgent issues and the potential for a

* Corresponding author. Tel.: +86 10 64807520; fax: +86 10 64807381.
E-mail address: tienpo@sun.im.ac.cn (P. Tien).

0166-3542/$ - see front matter © 2012 Elsevier B.V. All rights reserved.
http://dx.doi.org/10.1016/j.antiviral.2012.08.003

HFMD pandemic in the future prompted us to explore a more effective approach to combating these highly virulent viruses.

RNA interference (RNAi) is an evolutionarily conserved mechanism of sequence-specific, post-transcriptional gene silencing triggered by double-stranded RNAs (dsRNAs) (Fire et al., 1998). Over the last few years, numerous studies have demonstrated that the RNAi technique can be exploited as a potential therapeutic strategy to fight against infectious diseases by targeting viral transcripts and/or host genes which produce co-factors critical for virus replication, such as influenza virus A (Zhou et al., 2007), influenza virus B (Gao et al., 2006), human immunodeficiency virus type 1 (HIV-1) (Jacque et al., 2002; Liu et al., 2007), hepatitis B virus (HBV) (Li et al., 2004; Giladi et al., 2003), hepatitis C virus (HCV) (Yokota et al., 2003) and respiratory syncytial virus (Bitko et al., 2005). This approach has also been used successfully against viruses of the *Picornaviridae* family, including poliovirus (Gitlin et al., 2002; Haasnoot et al., 2007), rhinovirus (Phipps et al., 2004) as well as Coxsackievirus B 3 (Yuan et al., 2005). The success of RNAi has been widely reported in *in vitro* systems and has gradually led to growing interest in *in vivo* applications, and could eventually lead to its validation as a potential drug therapy for use against infectious diseases.

RNA viruses appear to be attractive targets for RNAi since their genomes function as both messenger RNAs as well as the RNA replication templates. Thus, the RNAi strategy has a great potential for being developed as an antiviral therapy against EV 71 and CA 16. Although it has been reported that RNAi could effectively inhibit EV 71 replication (Lu et al., 2004; Sim et al., 2005; Tan et al., 2007; Wu et al., 2008, 2009), the siRNAs selected in these studies did not show a broad-spectrum antiviral effect. To limit escape mutants, all the siRNAs targets designed in this study were conserved among most EV 71 and CA 16 China strains. This study is also the first report of using minicircle vector-derived siRNAs for interfering with EV 71 and CA 16 replication in host cells and animal infection models.

One of the most important objectives in gene therapy is to develop safe and efficient systems for gene transfer in eukaryotic cells. There are two main strategies: viral and non-viral based systems (Lyon et al., 2008). Although viral based systems have shown high transfection efficiencies *in vivo*, they have serious disadvantages, such as immunogenicity and inflammatory responses (Marshall, 1999). Non-viral gene delivery strategies are usually based on plasmid DNA carrying the gene of interest. Conventional plasmid vectors consist of a bacterial plasmid backbone and a transcription unit. However, these sequences may cause undesirable effects such as the production of antibodies against bacterial proteins expressed from cryptic upstream eukaryotic expression signals, changes in eukaryotic gene expression caused by the antibiotic resistance marker, and immune responses to CpG sequences (Jechlinger, 2006). Compared to conventional plasmids, minicircle vectors (MC) are novel forms of supercoiled DNA molecules designed for non-viral gene transfer. They have neither a bacterial origin of replication nor an antibiotic resistance gene and are generated in *E. coli* by site-specific recombination. Minicircles are superior to standard plasmids in terms of biosafety, improved gene transfer, and potential bioavailability. The efficiency of gene transfer with minicircle vectors has been evaluated both *in vitro* in transformed primary cells and *in vivo* in liver, muscle and experimental tumors (Darquet et al., 1997, 1999; Bigger et al., 2001; Chen et al., 2003, 2004). However, to date, minicircle vectors have not been applied in antivirus gene therapy. In this study, a novel minicircle vector based RNAi system was developed as a therapeutic approach to inhibiting EV 71 and CA 16 replications. Viral RNA, viral proteins, virus titer and cytopathic effects of the infected RD cells were examined and used as the indicators of targeted gene silencing. We demonstrated that siRNAs targeting the $3C^{pro}$ and $3D^{pol}$ of EV 71 and CA 16 genomes are capable of inhibiting the replication of these viruses. This study also showed that improvements in triggering RNAi could be achieved by the use of minicircle vectors for therapeutic treatments against HFMD.

2. Materials and methods

2.1. Cell cultures and virus assays

Rhabdomyosarcoma (RD) cells were propagated and maintained in Minimum Essential Medium (MEM) (Gibco, Invitrogen, USA) supplemented with 10% FBS (Gibco, Invitrogen, USA) at 37 °C with 5% CO_2.

The EV 71 strain Hubei-09 (GenBank accession No. GU434678.1) was obtained from State Key Laboratory of Virology, College of Life Sciences, Wuhan University, Wuhan, People's Republic of China. The CA 16 strain Shzh05-1 (GenBank accession No. EU262658.1) was obtained from the Institute of Pathogen Biology, Chinese Academy of Medical Sciences, Beijing, People's Republic of China. The two virus strains were propagated in RD cells. The 50% tissue culture infective dose ($TCID_{50}$) was calculated for RD cells by using 96-well plate and the Reed-Muench formula (Yuan et al., 2005).

2.2. Minicircle vector construction

The human RNA polymerase (Pol) III H1 promoter and U6 promoter, the latter containing 27 additional nucleotides upstream of the specific hairpin, were used in this study. The cassette containing the human U6 promoter and H1 promoter prepared from the pSuper-H1 + U6 plasmid preserved in our lab by digestion with BamHI and EcoRI was cloned into the same restriction sites of the parental minicircle vector pMC.BESPX-MCS2 (SBI, USA) to obtain the plasmid pMC-H1 + U6.

Conserved regions between the genomes of EV 71 and CA 16 China strains were obtained by alignment using SeqMan program (DNAStar, USA). The siRNAs based on these conserved regions were designed using the web-based siRNA tool BLOCK-iT™ RNAi Designer of Invitrogen and siRNA Target Finder of Ambion. A negative control for interfering with the Enhanced Green Fluorescent Protein (EGFP) gene which does not belong to the viral or host genes was designed. Each one of the siRNAs serves as a basis for the design of the two complementary siRNA template oligonucleotides. To facilitate the formation and processing of shRNAs, a loop sequence (TTCAAGAGA) was designed in the middle area of all shRNAs. Finally, nine pairs of complementary oligonucleotides targeting specific sequences in the 5′UTR, $3A^{pro}$, $3C^{pro}$, $3D^{pol}$, VP_1, VP_2 and VP_3 genes of EV 71 and CA 16, respectively, were custom synthesised by Invitrogen. The synthetic oligonucleotides were annealed to produce DNA duplexes and cloned into the BglII–SalI sites located between the U6 promoter and the H1 promoter to produce the respective recombinant vectors (pMC-H1 + siRNA + U6). Their fidelity was confirmed by DNA sequencing.

2.3. Production and purification of minicircles

ZYCY10P3S2T *E. coli* strain (SBI, USA) was transformed with the parental plasmids (pMC-H1 + siRNA + U6). A single colony from each transformation was grown in LB for 6–8 h at 37 °C. Then 100 μl of each culture was combined with 400 ml of fresh TB (Terrific Broth) containing 50 μg/ml kanamycin in a 2 l flask and cultured at 37 °C overnight (until OD600 = 4.5–5.0), with shaking at 250 rpm. Subsequently, 400 ml of fresh Luria–Bertani Broth containing 16 ml 1 N NaOH and 1.0% L-arabinose was added to each of the cultures and the bacteria cultivated for 5 h at 30 °C, with

shaking at 250 rpm. This activates the restriction enzyme I-SceI which cuts and linearizes the bacterial backbone plasmids and subjects them to degradation. Supercoiled MC DNA was isolated from the cultures using plasmid purification kits from the Qiagen (Hilden, Germany).

2.4. MC-siRNAs transfection and virus infection of RD cells

RD cells were seeded into 12-well plates and cultured at 37 °C with 5% CO_2. When the cell layers reached 60–70% confluency, the culture medium was changed to Opti-MEM I (Gibco, Carlsbad, CA) at 1 ml/well. The cells were transiently transfected with 1 μg MC-siRNAs by using 2 μl Lipofectamine 2000 (Invitrogen, USA) according to the manufacturer's recommendation. The culture medium was changed to MEM at the end of the transfection period (5–6 h) and the cells were infected with EV 71 (MOI 0.01) or CA 16 (MOI 0.02) as required. Viral RNA and protein production, virus titer and morphological changes in the RD cells were assessed at 48 h post-infection.

2.5. In vivo animal experiments with MC-siRNAs

One day old ICR suckling mice obtained from the Institute of Genetics and Developmental Biology, Chinese Academy of Sciences (CAS), Beijing were used in all *in vivo* experiments. All animal experiments were undertaken within the CAS guidelines and regulations for the use of experimental animals. The suckling mice were first infected with 10^7 $TCID_{50}$ of EV 71 via intra-peritoneal inoculation (IP). At 24 h post infection, the mice were treated with 20 μg of MC-siRNAs or phosphate-buffered saline (PBS) by IP. A parallel group of suckling mice not infected with EV 71 was used as negative controls. During the experiment, weights and clinical signs of all the suckling mice were monitored every alternate day for two weeks. The clinical score was graded as follows: 0, healthy; 1, lethargy and anorexia; 2, ruffled hair and hunched posture; 3, emaciation; 4, paralysis in hind limbs; and 5, death. Two weeks post-infection, the intestines were harvested from the suckling mice. The extracted intestines were stored at −80 °C until required for testing.

2.6. Real-time reverse transcription (RT)-PCR

Viral genome RNA was extracted from the supernatant of cells in each well by using QIAamp Viral RNA Mini Kit (QIAGEN, Hilden, Germany) according to the manufacturer's instructions. Total RNA was extracted from cells or tissues using TRIzol (Invitrogen, USA). Reverse transcription was carried out in a 10 μl reaction mixture with 500 ng RNA using the GoScript™ Reverse Transcription System (Promega, Madison, WI, USA) according to the manufacturer's protocol. Real-time fluorescence quantitative PCR was conducted using the ABI Prism 7300 Real-time PCR system (Applied Biosystems) in a 20 μl reaction volume containing 1 μl cDNA, 0.6 μl of each primer, 0.4 μl ROX™ passive reference dye and 10 μl SYBR Green Master Mix (Applied Biosystems). The reagents were denatured at 95 °C for 10 min, followed by 40 cycles of 10s at 95 °C and 60s at 60 °C. The following primers were used for the above RT-PCR:

EV 71 forward 5′-AGTATGATTGAGACTCGGTG-3′;
EV 71 reverse 5′-GCGACAAAAGTGAACTCTGC-3′;
CA 16 forward 5′-GGAAATGCGAGTTGTTTACCT-3′;
CA 16 reverse 5′-GGGGACTGACACTTGAGCTG-3′;
hGAPDH forward 5′-ACAGTCAGCCGCATCTTCTT-3′;
hGAPDH reverse 5′-GTTAAAAGCAGCCCTGGTGA-3′;
mGAPDH forward 5′-AGGTCGGTGTGAACGGATTTG-3′;
mGAPDH reverse 5′-TGTAGACCATGTAGTTGAGGTCA-3′.

PCR products amplified from the EV 71 and CA 16 RNAs were cloned into the pMD19-T Easy vector to produce plasmids which were used to constuct standard curves. Viral RNA in each test sample was then quantified using these standard curves. A melting curve analysis was performed to verify the authenticity of the amplification. Average Ct values for CA 16 and EV 71 were calculated and normalized to the Ct values for GAPDH. The normalized values were subjected to a $2^{-\Delta\Delta Ct}$ formula to calculate the fold change between the control and experiment groups. The formula and its derivations were obtained from the ABI Prism 7300 Sequence Detection System user guide. All reactions were performed in triplicates.

2.7. Western blotting assay

Viral proteins were extracted from RD cells or tissues with lysis buffer containing 50 mM Tris–HCl (pH 8.0), 1% NP-40, 15 mM NaCl and Protease Inhibitor Cocktail (1:1000) (Sigma–Aldrich, St. Louis, MO, USA). Protein concentration of each sample was measured by the Bradford method (Bio-Rad Laboratories, Hercules, CA, USA). Protein extracts were heat denatured at 100 °C for 8 min, electrophoretically separated on a 15% SDS–PAGE, and transferred to a polyvinylidene fluoride membrane. The membrane was blocked with 5% non-fat dry milk in TBS-T buffer (50 mM Tris–HCl, 100 mM NaCl and 0.1% Tween-20, pH 7.6) overnight and then incubated with monoclonal anti-EV 71 antibody (also cross-reacts with CA 16) at 1:2000 dilution (Millipore, Billerica, MA, USA), monoclonal anti-GAPDH at 1:2000 dilution (Zhongshan Bio-tech Ltd., Zhongshan, China) for a further 60 min at 37 °C. The signals were visualized by chemoluminescence reactions using horseradish peroxidase conjugated IgG (1:2000 dilution) in the ECL system (Amersham, Bucks, UK). The images and data were analyzed using the Quantity One® Version 4.6.2 program (Bio-Rad Laboratories, USA).

2.8. Cell viability assay

To assay for cell viability in the presence of MC-siRNAs, RD cells were seeded in a 96-well plate and the transfections of cells were performed as described above. At 48 h post-transfection, 20 μl of the MTS/PMS reagent (Promega, USA) was added into each well to measure the absorbance at 490 nm according to the manufacturer's recommendations. All assays were performed in triplicates and repeated in a second independent experiment.

2.9. IFN-α and IFN-β assay

RD cells seeded in 24-well plates were transfected as described above. At 48 h post-transfection, the levels of IFN-α and IFN-β in the culture supernatants of cells were measured using an ELISA kit (PBL Biomedical Laboratories, Piscataway, NJ) according to the manufacturer's instructions.

2.10. Histological analysis

Two weeks post infection, the intestines and brains were removed from the suckling mice and either fixed in formalin and embedded in paraffin. Paraffin sections (2–4 μm) were stained with hematoxylin and eosin. Measurement of histopathological changes was performed by pathologists in a blind manner.

2.11. Statistical analysis

Data are expressed as means ± SD. Statistical tests between two experimental groups were performed by independent-samples *T* tests using the SPSS statistical package. *P* values <0.05 were considered significantly different.

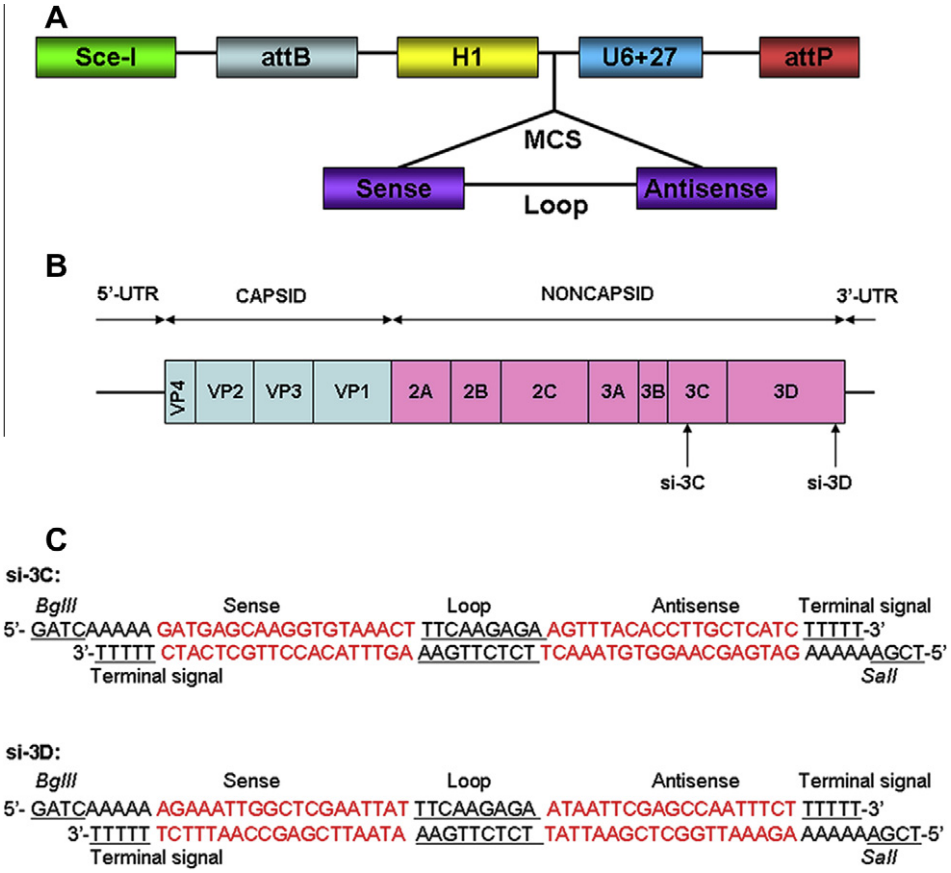

Fig. 1. Minicircle vector-mediated RNA interference. (A) Schematic representation of the minicircle plasmid vector pMC-H1 + siRNA + U6 construct containing components attB, bacterial attachment site; attP, phage attachment site; Sce-I, endonuclease site; MCS, multiple cloning sites; siRNA coding template containing sense, loop and antisense sequences, and the H1 and U6 promoters. (B) Schematic representations of the EV 71/CA 16 RNA structure showing the siRNA target sites on the 3C and 3D genes. (C) DNA sequences of the si-3C and si-3D siRNA constructs showing the siRNA DNA templates in red. (For interpretation of the references to color in this figure legend, the reader is referred to the web version of this article.)

3. Results

3.1. Optimization of the minicircle vector system for siRNA delivery

A recombinant minicircle plasmid was constructed to drive high levels of transient expression of the small hairpin RNA (shRNA) under the direction of both the RNA Pol III promoter of human U6 and the H1 small nuclear RNA promoter inserted in reverse orientation to each other (Fig. 1A). The configuration of the constructs and the sequences of the inserted oligonucleotides targeting the 5′UTR, $3A^{pro}$, $3C^{pro}$, $3D^{pol}$, VP_1, VP_2 and VP_3 genes of both EV 71 and CA 16 were confirmed by DNA sequencing (Table 1). To test the effects of these siRNAs on the replication of EV 71 and CA 16 *in vitro*, virus-infected RD cell line was transfected with the MC-siRNAs with the aid of Lipofectamine. When the transfected cells were analyzed for transfection and expression efficiencies using a minicircle DNA

Table 1
Chemically synthesised siRNA DNA oligonucleotides inserted into pMC-H1 + U6.

siRNAs	DNA oligonucleotide sequences
si5′UTR-190 sense	5′-GATCAAAAA GACTGAGTATCAATAGACT TTCAAGAGA AGTCTATTGATACTCAGTC TTTTT-3′
si5′UTR-190 antisense	5′-TCGAAAAAA GACTGAGTATCAATAGACT TCTCTTGAA AGTCTATTGATACTCAGTC TTTTT3′
si5′UTR-611 sense	5′-GATCAAAAA GTTGTTACCATATAGCTAT TTCAAGAGA ATAGCTATATGGTAACAAC TTTTT-3′
si5′UTR-611 antisense	5′-TCGAAAAAA GTTGTTACCATATAGCTAT TCTCTTGAA ATAGCTATATGGTAACAAC TTTTT-3′
siVP1-3190 sense	5′-GATCAAAAA GGTGTATATGAGGATTAAA TTCAAGAGA TTTAATCCTCATATACACC TTTTT-3′
siVP1-3190 antisense	5′-TCGAAAAAA GGTGTATATGAGGATTAAA TCTCTTGAA TTTAATCCTCATATACACC TTTTT-3′
siVP2-997 sense	5′-GATCAAAAA TTACCATTGGAAATTCCAC TTCAAGAGA GTGGAATTTCCAATGGTAA TTTTT-3′
siVP2-997 antisense	5′-TCGAAAAAA TTACCATTGGAAATTCCAC TCTCTTGAA GTGGAATTTCCAATGGTAA TTTTT-3′
siVP3-1832 sense	5′-GATCAAAAA GTACGCAACCTATTGGAAA TTCAAGAGA TTTCCAATAGGTTGCGTAC TTTTT-3′
siVP3-1832 antisense	5′-TCGAAAAAA GTACGCAACCTATTGGAAA TCTCTTGAA TTTCCAATAGGTTGCGTAC TTTTT-3′
si3A-5279 sense	5′-GATCAAAAA GTGTCTCTTGTCTATGTCA TTCAAGAGA TGACATAGACAAGAGACAC TTTTT-3′
si3A-5279 antisense	5′-TCGAAAAAA GTGTCTCTTGTCTATGTCA TCTCTTGAA TGACATAGACAAGAGACAC TTTTT-3′
si3C-5577 sense	5′-GATCAAAAA GATGAGCAAGGTGTAAACT TTCAAGAGA AGTTTACACCTTGCTCATC TTTTT-3′
si3C-5577 antisense	5′-TCGA AAAAA GATGAGCAAGGTGTAAACT TCTCTTGAA AGTTTACACCTTGCTCATC TTTTT-3′
si3C-5701 sense	5′-GATCAAAAA GAGCACATGCCCTCAATGT TTCAAGAGA ACATTGAGGGCATGTGCTC TTTTT-3′
si3C-5701 antisense	5′-TCGA AAAAA GAGCACATGCCCTCAATGT TCTCTTGAA ACATTGAGGGCATGTGCTC TTTTT-3′
si3D-7302 sense	5′-GATCAAAAA AGAAATTGGCTCGAATTAT TTCAAGAGA ATAATTCGAGCCAATTTCT TTTTT-3′
si3D-7302 antisense	5′-TCGAAAAAA AGAAATTGGCTCGAATTAT TCTCTTGAA ATAATTCGAGCCAATTTCT TTTTT-3′
siEGFP sense	5′-GATCAAAAAAGAACGGCATCAAGGTGAACTTCAAGAGAGTTCACCTTGATGCCGTTCTTTTTT-3′
siEGFP antisense	5′-TCGAAAAAAAGAACGGCATCAAGGTGAACTCTCTTGAA GTTCACCTTGATGCCGTTCTTTTTT-3′

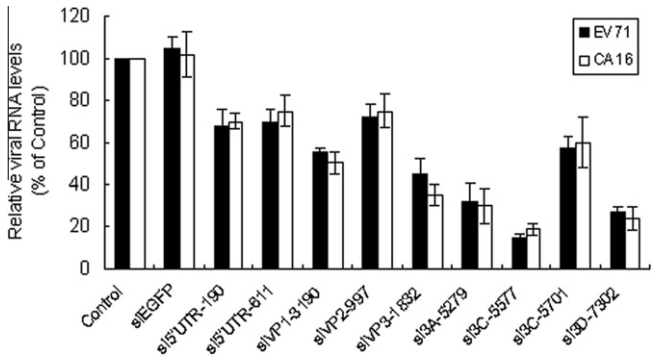

Fig. 2. Bar diagram showing the antiviral effects of nine siRNA-encoding minicircle vectors (*x*-axis) on CA 16 and EV 71 viral RNA levels. Viral RNA levels, expressed % control, were obtained using real-time RT-PCR at 48 h post-infection. The plotted data were averages from triplicate samples.

expressing EGFP, approximately 80% of cells were transfected as measured by FACS analysis (data not shown). This confirmed that the minicircle-based system was a highly efficient gene delivery system. The siRNA constructs that were most effective in inhibiting virus replication was identified by Real time PCR analysis of EV 71 and CA 16 RNA expression in RD cells. The results showed that si3C-5577 and si3D-7302 could significantly down regulate the expression of viral RNA (Fig. 2). DNA oligonucleotides consisting of sense and antisense sequences encoding si3C-5577 with a target site in the 3C mRNA (5′-GATGAGCAAGGTGTAAACT-3′) and si3D-7302 with a target site in the 3D mRNA (5′- AGAAATTGGCTCGAATTAT-3′) were cloned between the H1 promoter and U6 promoter to construct the recombinant minicircle vector, using a loop structure sequence TTCAAGAGA and five thymidines as the terminal signal (Fig. 1B and C). They were selected for subsequent *in vitro* and *in vivo* studies.

Production of minicircles required a special parental plasmid (PP) and an engineered *E. coli* strain that allowed both the propagation of the parental plasmid and the production of the minicircles. Minicircles were conditionally generated by expressing an inducible ΦC31 integrase via intramolecular (cis-) recombination between *att*B and *att*P. The full-size MC-DNA construct was grown in a special host *E. coli* strain that harbored an arabinose-inducible system to express the ΦC31 integrase and the SceI endonuclease simultaneously. The ΦC31 integrase produced the MC-DNA molecules expressing the shRNAs and the plasmid bacterial backbone (BB) DNA from the full-size MC-DNA upon arabinose induction. The BB-DNA contained a number of engineered SceI restriction

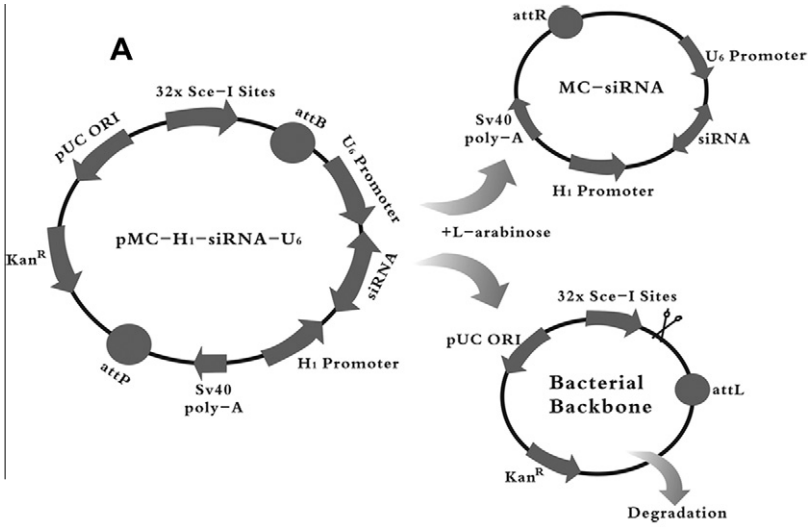

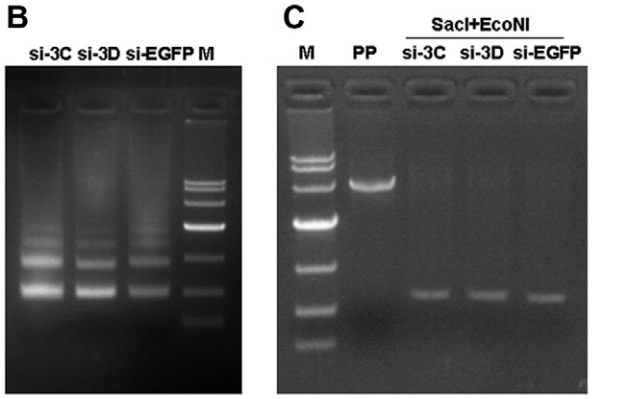

Fig. 3. Production of minicircle-siRNA vectors from the pMC-H1 + siRNA + U6 plasmids. (A) Flow chart of ΦC31 integrase-mediated intramolecular recombination of pMC-H1 + siRNA + U6 in the presence of L-rabinose producing two circular DNAs. One was MC-siRNA containing the siRNA cassette and the right hybrid sequence (*att*R) that was the product of site-specific recombination between the *att*B and *att*P sites driven by bacteriophage ΦC31 integrase. The other was the bacterial backbone which contains the origin of replication, the antibiotic marker, and the left hybrid sequence (*att*L). This bacterial backbone plasmid was linearized by SceI homing endonuclease and was removed by bacterial exonucleases. (B) Purity analysis of minicircle siRNA vector preparations by agarose gel electrophoresis. The results confirmed the formation of minicircles and destruction of most of the plasmid bacterial backbone. Lanes si-3C, si-3D and si-EGFP represent minicircle vector DNAs carrying siRNAs expression cassettes targeting $3C^{pro}$, $3D^{pol}$ and EGFP, respectively. M, Marker (DL-10000). (C) Quality analysis of the resulting MC-siRNA vectors in agarose gel. The MC-siRNAs digested with *Sac*I and *Eco*NI produced predominantly a 0.6-kb band representing the minicircle. PP, parental plasmid. Labeling are the same as in (B).

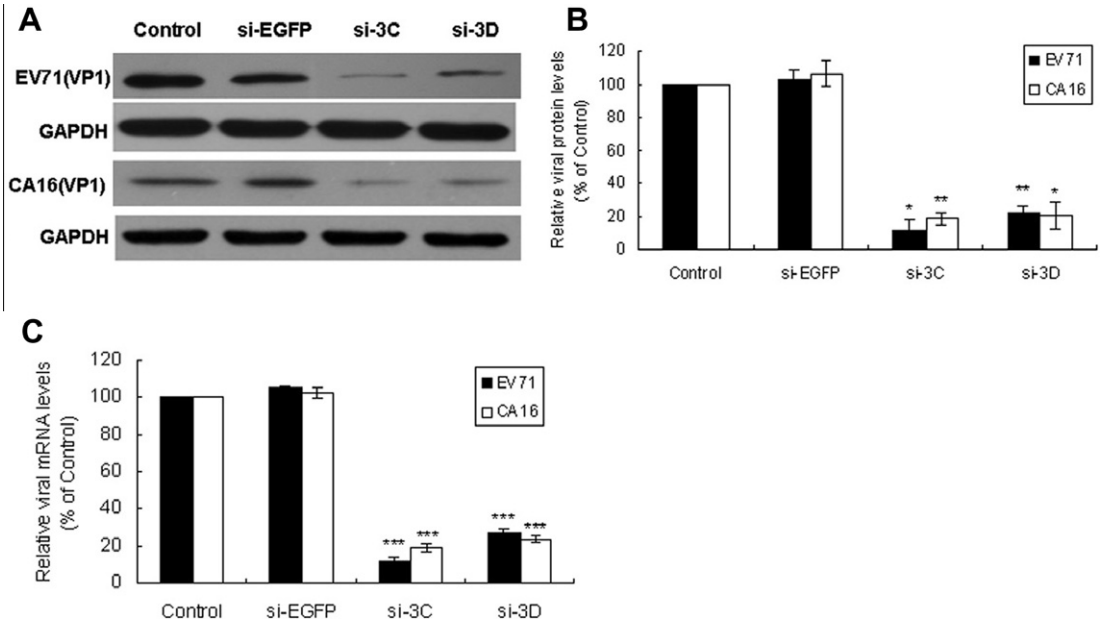

Fig. 4. Analysis of inhibition of EV 71 and CA 16 gene expression in RD cell line by RNAi based on minicircle delivery. Lanes si-3C, si-3D and si-EGFP represent samples from cells transfected with minicircle vector DNAs carrying siRNAs expression cassettes targeting $3C^{pro}$, $3D^{pol}$ and EGFP, respectively. Control lanes contained samples from cells transfected with PBS. (A) Analysis of the effect of siRNAs on viral protein expression level by Western blot. (B) Quantitation of viral protein levels obtained from the western blots. (C) Analysis of the effect of siRNAs on viral mRNA expression level by real-time RT-PCR. All the data presented were the mean ± SD obtained from three independent experiments. $^{*}p < 0.05$, $^{**}p < 0.02$, $^{***}p < 0.001$.

sites that were subjected to digestion by SceI endonuclease, and ultimately it own destruction. The MC-DNA lacked SceI restriction sites so that it remained intact.

The 32 copies of SceI sites in the plasmid bacterial DNA ensured the production of MC-DNA without BB-DNA contamination (Fig. 3A). The purity of MC-siRNA was analyzed by agarose gel electrophoresis (Fig. 3B) which showed that PP-DNA and BB-DNA contamination were weak and barely detectable. This result confirmed the formation of minicircle and the destruction of most of the plasmid bacterial backbone. We also examined the quality of the resulting MC-siRNA by comparing the migration patterns of cut and uncut samples in agarose gels. MC-siRNA digested with *Sac*I and *Eco*NI produced predominantly a 0.6 kb band representing the minicircle (Fig. 3C). The results indicated that most of the MC-siRNA was supercoiled with small amounts of nicked, linear and dimeric forms.

3.2. Interference of EV 71 and CA 16 replication by si3C and si3D in cultured cells

RD cells were infected respectively with EV 71 and CA 16 after being transfected with si3C and si3D recombinant minicircle DNAs and the negative control. Western blotting was then performed to measure the viral protein expression levels in the infected cells (Fig. 4A). The results showed that the protein levels of EV 71 and CA 16 were significantly reduced, down to 10.8 ± 6.7% and 18.5 ± 4.0% of controls, respectively, in si3C recombinant minicircle-transfected cells, and to 22.1 ± 4.2% and 20.6 ± 8.6% of controls, respectively, in si3D recombinant minicircle-transfected cells, whereas no inhibiting effect was observed in cells transfected with the siEGFP minicircle vector (Fig. 4B). To see whether si3C and si3D also caused a reduction in viral mRNA levels, real time reverse transcription PCR analysis was performed on total RNAs extracted from RD cells infected with EV 71 or CA 16. The results showed that si3C and si3D significantly reduced EV 71 and CA 16 mRNAs levels such that mRNA level of EV 71 was 12.4 ± 1.7% and that of CA 16 was 19.2 ± 2.0% of controls in cells transfected with MC-si3C, and mRNA level of EV 71 was 27.4 ± 2.2% and that of CA 16 was 23.9 ± 1.6% of controls in cells transfected with MC-si3D (Fig. 4C). These data confirmed that the minicircle-delivered shRNAs efficiently inhibited the gene expression of these viruses in RD cells.

3.3. Interference of EV 71 and CA 16 virus production by si3C and si3D in cultured cells

To ascertain whether MC-siRNAs-mediated inhibition of intracellular viral protein and mRNA production also affected the generation of progeny viruses, supernatants from the infected cell lines were collected and analyzed for the amounts of viral genomes and virus particles produced. Real time reverse transcription PCR analysis of RNAs extracted from the supernatants revealed that the copy numbers of extracellular viral genomes of both viruses dropped significantly, down to 8.5% of control for EV 71 and 10.2% of control for CA 16 in cells transfected with MC-si3C. Similarly, extracellular viral genomic RNAs dropped to 15.0% of control for EV 71 and 12.1% of control for CA 16 in cells transfected with MC-si3D (Fig. 5A). Virus titers in the supernatants were measured to quantify the inhibitory activities. As shown in Fig. 5B, virus titers of the negative controls were markedly higher than those of the MC-si3C transfected cells which showed a 62.2-fold reduction in the EV 71 infected cells and a 48.6-fold reduction in the CA 16 infected cells. Comparatively, MC-si3D caused a 38.3-fold reduction in virus titers in EV 71 infected cells and a 41.0-fold reduction in CA 16 infected cells. The levels of inhibition of extracellular genomic RNA and progeny virus production corresponded well with the potency of MC-siRNAs in reducing the amount of intracellular viral proteins and mRNAs. In addition, examination of morphological changes in RD cells using phase-contrast microscopy revealed a remarkable resistance to damage by EV 71 and CA 16 in cells pre-transfected with si3C or si3D recombinant minicircle DNA. This was in sharp contrast to cells treated with the control siEGFP minicircle DNA which showed approximately 100% CPE (Fig. 5C and D). The results showed that the minicircle based siRNA system was able to inhibit EV 71 and CA 16-induced CPE in RD cells.

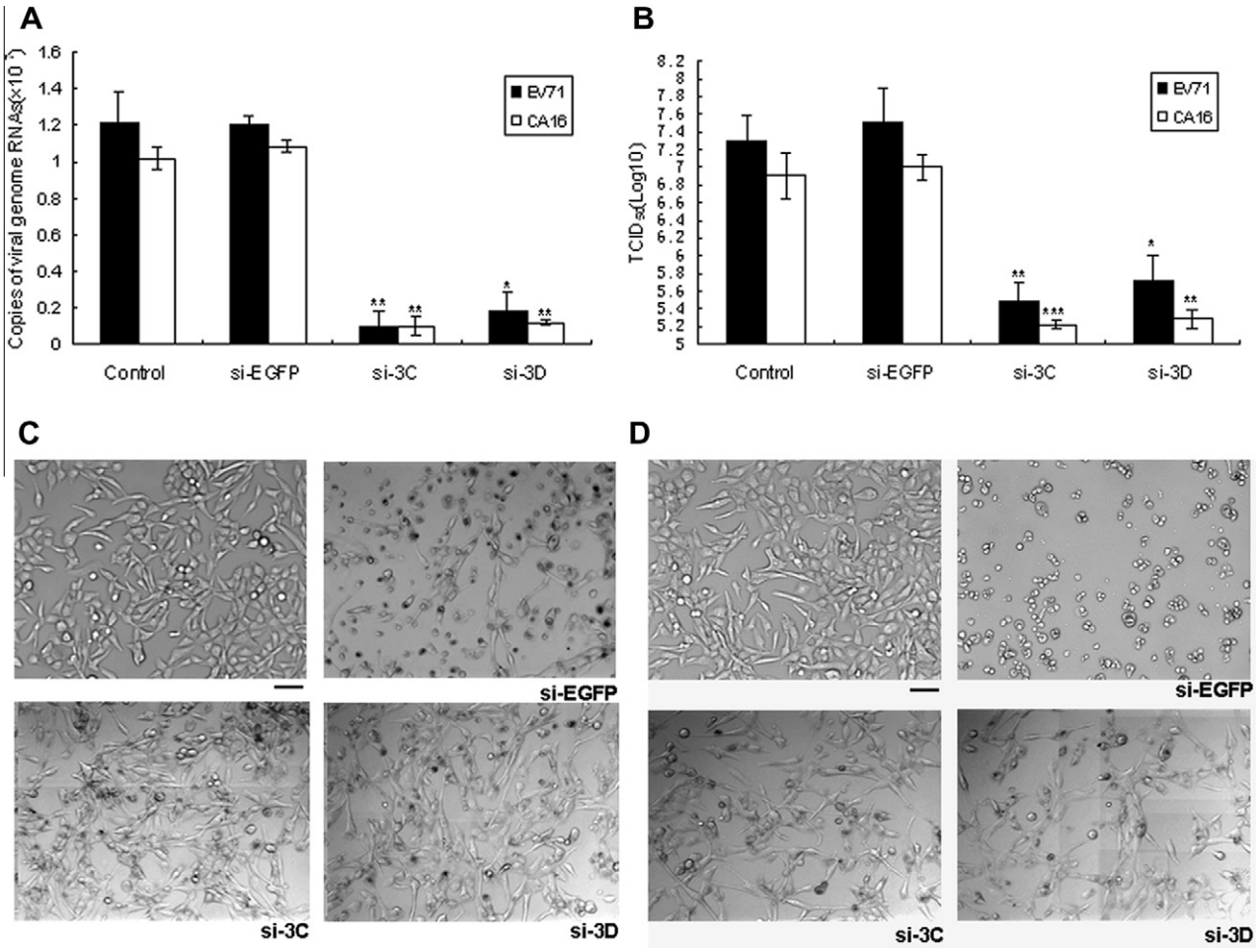

Fig. 5. Analysis of inhibition of EV 71 and CA 16 virus replication in RD cell line by RNAi based on minicircle delivery. RD cells were treated as described in Fig. 4. (−) = health cell control. Where indicated, all data shown were mean ± standard deviations obtained from three independent experiments. $^{*}p < 0.05$, $^{**}p < 0.02$,$^{***}p < 0.001$. (A) Viral RNAs were isolated from the cells 48 h post-infection. The number of copies of viral genomic RNAs in each sample was calculated from real-time RT-PCR assays. (B) Culture supernatants of the cells were taken and TCID50 values were determined 48 h post-infection. (C) Analysis of morphological changes in RD cells caused by EV 71 when pre-transfected with shRNA-encoding minicircle vectors at 48 h post-infection. (D) Analysis of morphological changes in RD cells caused by CA 16 at 48 h post-infection.

3.4. Specificity and cytotoxicity analysis of the minicircle RNAi system

To verify that the virus inhibition by si3C and si3D was due to specific antiviral effects exerted by the minicircle mediated RNAi and not due to activation of IFNs, we measured the levels of IFN-α and IFN-β in the cultured cells. The results showed no activation of IFN-α or IFN-β and we therefore concluded that the virus inhibition was mediated specifically through MC-siRNAs (Fig. 6A).

To confirm that no cytotoxicity was induced by the siRNA-minicircle vectors, a MTS/PMS assay was carried out at 48 h post-transfection to measure the viability of cells. The results showed that the siRNA-minicircle system did not cause any cytotoxic effects affecting the growth and viability of RD cells (Fig. 6B).

3.5. Inhibition of EV 71 and CA 16 replication using a combined minicircle-mediated siRNAs

To test whether using a combination of the two siRNAs to target both the 3C and 3D genes simultaneously could enhance the antiviral activity, we constructed a minicircle vector MC-si3C + si3D by combining the si3C and si3D expression cassettes (Fig. 7A). As shown in Fig. 7B, MC-si3C + si3D reduced viral RNA production to 17.3 ± 2.5% of control in EV 71 infected cells and to 21.3 ± 5.3% of control in CA 16 infected cells. Similarly, when measured at 48 h post-infection, MC-si3C + si3D reduced the virus titers 52.0-fold in EV 71 infected cells and 46.2-fold in CA 16 infected cells (Fig. 7C and D). The inhibition of viral titer was observed to last for up to 72 h post-infection. However, no additive effect on antiviral activity was observed. These results confirmed that the combined minicircle mediated siRNAs could also effectively inhibit replication of EV 71 and CA 16 in RD cells.

Although there was no additional antiviral activity by using the combined siRNAs in this study, we consider this could be a better strategy than using a single siRNA because it could reduce the formation of viral resistant mutants. A combination of siRNAs targeting multiple conserved regions of EV 71 and CA 16 nucleotide sequences could sufficiently protect patients against EV 71 and CA 16 and this strategy may also conceive siRNA drugs that could inhibit most EV 71 and CA 16 China strains.

The siRNAs dose response of viral suppression were studied using MC-si3C/3D in RD cells. As shown in Fig. 7E, transfection of RD cells with MC-si3C/3D resulted in inhibition of EV 71 RNA by 60%, 76%, 83% when the dosages of si3C/3D were 100,500,and 1000 ng. Similar dosage dependency effects were observed in the cells infected with CA 16 (53%, 70% and 79%). These results indicated that MC-siRNA exerted potent antiviral activity in a dose dependent manner.

3.6. MC-siRNAs-mediated inhibition of EV 71 in vivo

To test the antiviral activity of MC-si3C + si3D, suckling mice were first infected with 10^7 $TCID_{50}$ of EV 71 by intraperitoneal

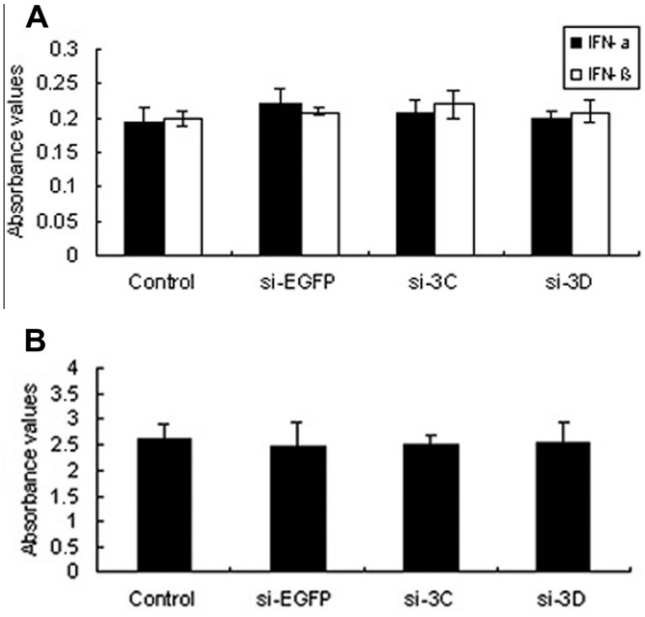

Fig. 6. Analysis of the specificity and cytotoxicity of the minicircle RNAi system. Experimental treatments were as described in Fig. 4. The data shown represented the mean ± SD calculated from two independent experiments. (A) Viability of RD cells (as an indicator of cytotoxicity) was determined by the MTS assay after transfection with MC-siRNAs. Absorbance values of the cells were measured at 490 nm. (B) The levels of IFN-α and IFN-β in the cells were determined by measuring the absorbance values at 490 nm.

inoculation (IP). At 24 h post- infection, the infected mice were inoculated with 20 μg of MC-si3C + si3D, MC-siEGFP, or phosphate-buffered saline (PBS) by the same route. A separate group of suckling mice not infected with EV 71 was used as negative controls. Two weeks after EV 71 infection, the mice were assessed and the results showed that the suckling mice treated with MC-si3C + -si3D showed significant protection against EV 71 infection since they showed no signs of significant weight loss or acute flaccid paralysis of the hind limbs. In contrast, the mice that received no siRNA and those that were treated with siEGFP showed significant weight loss and hind limb paralysis from day 6 post-infection (Fig. 8A and B). Thus, MC-siRNA treatment significantly reduced morbidity and subsequent paralysis sequelae in infected mice. Two weeks post-infection, intestines were harvested from the suckling mice to assess the inhibitory effects of MC-siRNAs on EV 71 replication using real time RT-PCR and Western blot. It was observed that treatment with 20 μg of MC-si3C + si3D led to ~80% decrease in viral transcripts (Fig. 8E). Western blot of the EV 71 viral proteins in the intestines (Fig. 8C) showed that the VP1 viral protein levels decreased correspondingly (Fig. 8D) after MC-siRNA treatment. Thus, minicircle plasmids expressing shRNAs were able to inhibit EV 71 replication in a murine model.

3.7. Histological analysis of MC-siRNA-treated suckling mice

The effects of MC-siRNAs on pathological changes caused by EV 71 in sucking mice were assessed by histological analysis of the intestines and brains harvested from the mice two weeks post-infection. In the mice not treated with siRNAs, extensive damages to the intestines and brains were observed (Fig. 9). In these mice, intestinal villus interstitial edema and epithelial cell vacuolar degeneration were detected in the small intestines. Encephaledema and focal microglial cell hyperplasia were observed in the brains of EV 71 infected mice not treated with siRNAs. In contrast, no obvious pathological changes were observed in corresponding tissues harvested from infected mice that were treated with MC-si3C + si3D. These results highlighted the effectiveness of the minicircle vector-based RNAi system for its ability to inhibit EV 71 replication *in vivo*.

4. Discussion

EV 71 and CA 16 are the two major causative agents of HFMD in China. Serious complications arising from their infections can lead to rapid clinical deterioration and even death. The clinical symptoms caused by EV 71 are indistinguishable from those caused by CA 16. HFMD has become an emerging disease in China since March 2008 (Sim et al., 2005; Tan et al., 2007; Wu et al., 2008). Accumulated cases up to 2010 have reached 3.4 million, including nearly 1400 fatalities. It is important to note that most deaths from HFMD caused by them occur within 24 h, due to children developing complications associated with HFMD (Bible et al., 2008). So far there is no effective antiviral therapy or vaccine available to prevent or treat the severe complications caused by EV 71 and CA 16 infections.

Viral-vector derived siRNAs have been successfully employed for gene knockdowns. The need for specific delivery to the target cells can also be addressed by the use of viral-based vectors. However, the use of viral vectors is plagued with problems like immunogenicity and random integration into the host-genome, especially for adenoviral- and lentivirus-based vectors. Nonviral vectors have many advantages over viral systems, such as a better safety profile, the absence of theoretical size limitation for the expression cassette, and possibly simpler clinical translation attributable to easier good manufacturing practices. However, concerns have been raised regarding the lack of robust transfection efficiency and the immunostimulatory prokaryotic CpG motives in the bacterial backbone. To resolve these issues, we developed the novel nonviral minicircle vector based RNAi system that exhibited higher gene expression than the regular plasmid *in vitro*, as well significantly longer transgene expression *in vivo*. This drastic improvement is attributable to the removal of unnecessary plasmid sequences, which could affect the gene expression, and the smaller size of the MC, which might confer better extracellular and intracellular bioavailability and thus improved gene delivery properties (Darquet et al., 1997, 1999). In particular, the bacterial backbone sequences are often abundant with CpG islands, which can lead to transcriptional gene silence *in vivo*, and is one of the major reasons why regular plasmids are notoriously ineffective for long-term expression.

Experimentally, the RNAi technique has been extensively exploited as a specific and effective therapeutic strategy to fight against infectious diseases. This study showed that gene transfer mediated by the minicircle vector is a promising novel approach as an antivirus therapy and it possesses great potentials to fight against EV 71 and CA 16. The minicircle-derived siRNAs could also be considered as an economical alternative to chemical synthesis of siRNAs. Once the mode of induction is chosen, a delivery strategy must also be determined. The systemic administration approach was used in this study since EV 71 infections can affect multiple organs, including the intestines and the brain. The most commonly used routes of delivery among the *in vivo* studies are intravenous, subcutaneous, and intraperitoneal injections. For injection through different routes, delivery can be enhanced by encapsulation of the siRNAs in synthetic vehicles such as liposome, cationic polymers and nonionic polymers, etc. Moreover, siRNAs can be conjugated to targeting antibodies, peptides, or aptamers that target particular cell types or infected cells. The systems should provide efficient delivery of active siRNAs into target cells or tissues and target tissue-specific distribution after systemic

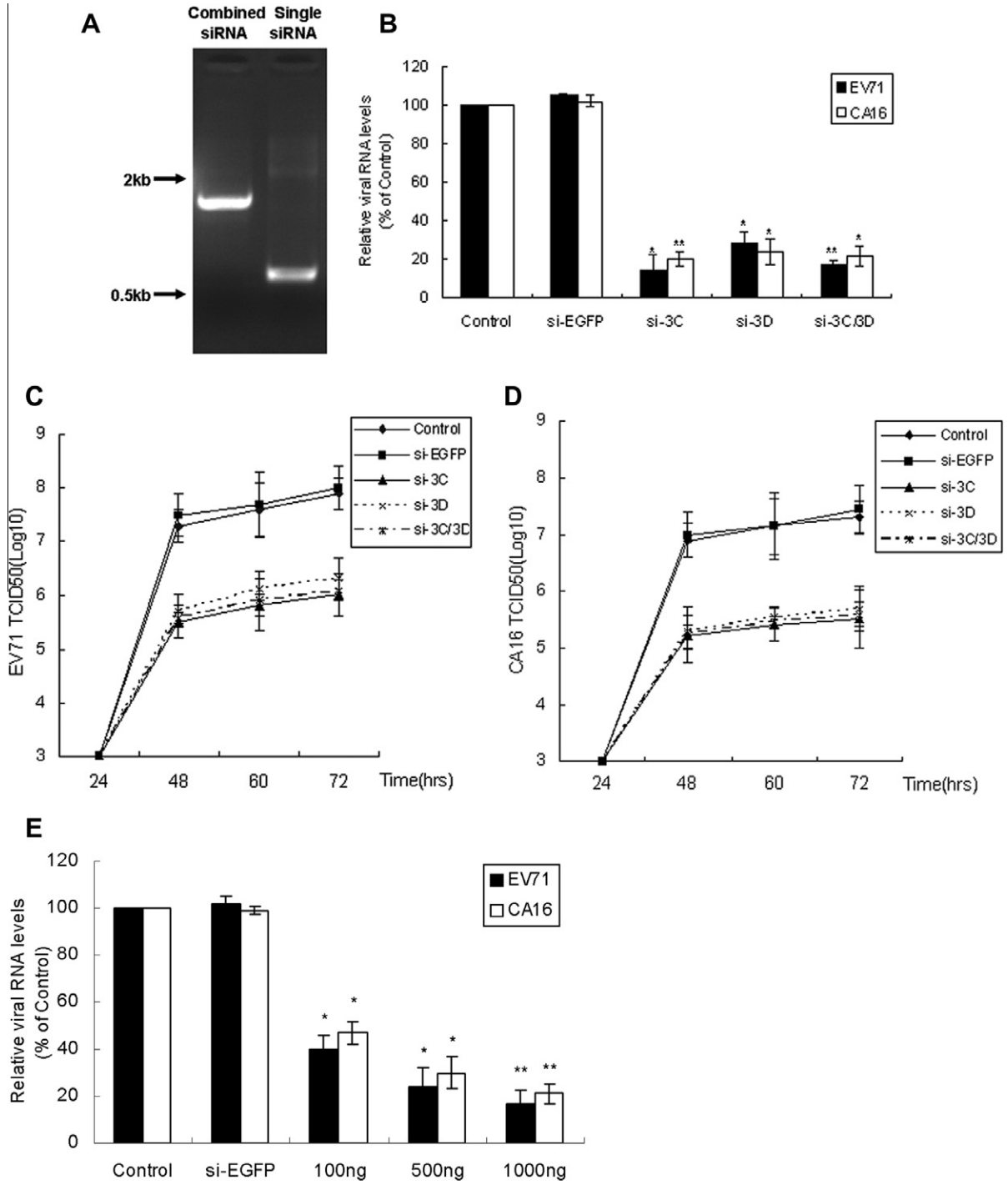

Fig. 7. Analysis of the inhibition of EV 71 and CA 16 replication by the combined siRNAs minicircle MC-si3C + si3D. Cells were treated as described in Fig. 4. In addition, another group was similarly treated with the combined siRNAs minicircle DNA. All data presented were the mean ± SD calculated from three independent experiments. $^{*}p < 0.05$, $^{**}p < 0.02$. (A) Analysis of MC-si3C + si3D produced by combining si3C and si3D expression cassettes in a single minicircle vector by agarose gel electrophoresis. Single siRNA, MC-si3C or MC-si3D; Combined siRNAs, MC-si3C + si3D. (B) Analysis of the effects of the combined siRNAs minicircle DNA on viral RNA levels in RD cells by quantitative RT-PCR. (C) EV 71 virus titers of the cell culture supernatants (TCID50) measured at 24, 48, 60 and 72 h post-infection and (D) CA 16 virus titers of the cell culture supernatants (TCID50) measured at 24, 48, 60 and 72 h post-infection. (E) Inhibition of viral RNA by different dosages of combined siRNAs minicircle MC-si3C + si3D. The RD cells were transfected with 100, 500 and 1000 ng of MC-si3C + si3D, followed by infections with EV 71 and CA 16. Viral RNAs were isolated from the cells 48 h post-infection and measured by quantitative RT-PCR.

administration. Therefore, further development of effective and safe systemic delivery approaches is necessary.

This study is the first report of using minicircle-derived siRNAs to interfere with EV 71 and CA 16 replication *in vitro* and *in vivo* and addressed a need to develop and test the effectiveness of minicircle-derived siRNA molecules as potent, specific inducers of RNA silencing, that would result in substantial abrogation of EV 71 and CA 16 replication. By targeting the non-structural genes of EV 71 and CA 16, our results produced four separate lines of evidence establishing that RNAi can be used to suppress EV 71 and CA 16 replications. These are: (1) minicircle-derived siRNAs significantly reduced viral RNA levels in infected cells and suckling mice; (2) EV

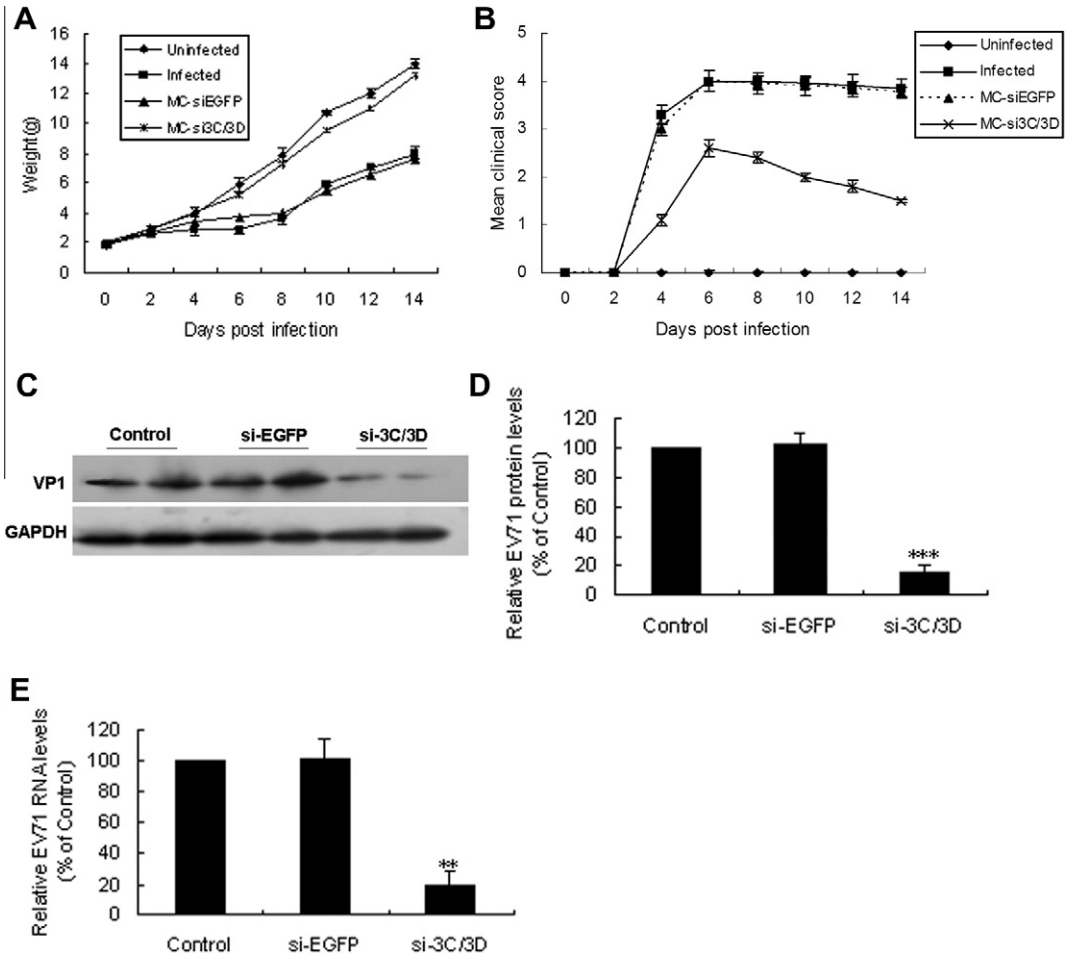

Fig. 8. Analysis of MC-siRNAs mediated inhibition of EV 71 replication in infected suckling mice. Infected suckling mice were treated with the following species of MC-siRNAs vectors as described in Materials and Methods. Controls in Panels (C–E) were the infected suckling mice treated with PBS. Where indicated, all data presented were the mean ± SD calculated from three independent experiments. (A) Changes in weights of uninfected or EV 71-infected mice treated with the indicated species of MC-siRNAs. (B) The clinical scores of mice were recorded. The clinical score was graded as follows: 0, healthy; 1, lethargy and anorexia; 2, ruffled hair and hunched posture; 3, emaciation; 4, paralysis in hind limbs; and 5, death. (C) Effect of the combined siRNAs minicircle DNA on viral protein levels in the intestines from the suckling mice as measured by Western blots. (D) Quantitation of the viral protein levels observed in the Western blots. (E) Effect of the combined siRNAs minicircle DNA on viral RNA levels in the intestines from the suckling mice as determined by quantitative RT-PCR assays.

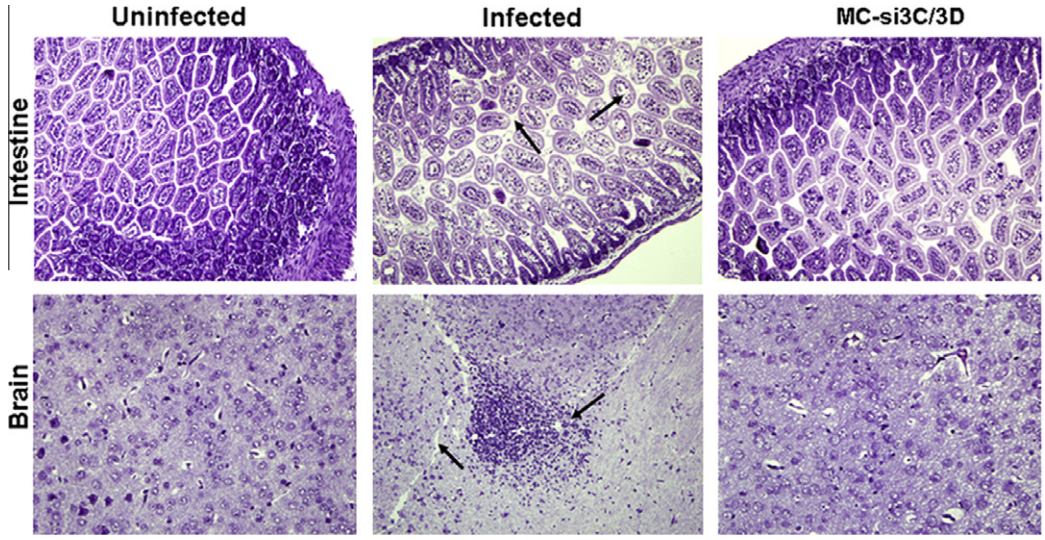

Fig. 9. Histological analysis of the treated suckling mice. The effects of MC-siRNAs on pathological changes of the intestines and brains harvested from the treated suckling mice were determined. Arrows indicated intestinal villus interstitial edema and epithelial cell vacuolar degeneration in the small intestines, encephaledema and focal microglial cell hyperplasia in the brains. The specimens shown are representative of 3 mice in each group with similar histology. Observations were made at a magnification of 200×.

71- and CA 16-specific protein (VP_1) was visibly reduced in infected cells and suckling mice treated with the siRNAs; (3) viral progeny multiplication as measured by $TCID_{50}$ assay was significantly reduced upon siRNAs treatment and (4) the cells transfected with the siRNAs were protected from the onset of cytopathic effects (CPE).

In conclusion, si3C and si3D targeting conserved regions of $3C^{pro}$ and $3D^{pol}$ were found to effectively inhibit the replication of EV 71 and CA 16. Nucleotide sequence analysis of the EV 71 and CA 16 genomes indicated that the observed anti-EV 71 and anti-CA 16 effects had profited from the conservation of the selected target sequences. Our results indicated that minicircle-derived siRNAs could be suitable for further development as an antiviral therapy against CA 16 and EV 71 strains.

Acknowledgements

This work is supported by grants from the National Basic Research Program of China (973 Program) (Nos. 2011CB504703 and 2010CB530102), the Major National Science & Technology Specific Projects of China (No. 2009ZX09103-747), and the National Science Foundation of China (NSFC, Grant No. 81021003). We are grateful to Prof. Paul Chu, guest professor of Institute of Microbiology, Chinese Academy of Sciences, for critical readings of the manuscript. We also thank Weihua Zhuang and Fulian Liao for their kind help with the experiments.

References

Alexander Jr., J.P., Baden, L., Pallansch, M.A., Anderson, L.J., 1994. Enterovirus 71 infections and neurologic disease—United States, 1977–1991. J. Infect. Dis. 169, 905–908.

Bible, J.M., Iturriza-Gomara, M., Megson, B., Brown, D., Pantelidis, P., Earl, P., Bendig, J., Tong, C.Y., 1998. Molecular epidemiology of human enterovirus 71 in the United Kingdom from 1998 to 2006. J. Clin. Microbiol. 46, 3192–3200.

Bigger, B.W., Tolmachov, O., Collombet, J.M., Fragkos, M., Palaszewski, I., Coutelle, C., 2001. An araC-controlled bacterial cre expression system to produce DNA minicircle vectors for nuclear and mitochondrial gene therapy. J. Biol. Chem. 276, 23018–23027.

Bitko, V., Musiyenko, A., Shulyayeva, O., Barik, S., 2005. Inhibition of respiratory viruses by nasally administered siRNA. Nat. Med. 11, 50–55.

Chan, K.P., Goh, K.T., Chong, C.Y., Teo, E.S., Lau, G., Ling, A.E., 2003. Epidemic hand, foot and mouth disease caused by human enterovirus 71, Singapore. Emerg. Infect. Dis. 9, 78–85.

Chen, Z.Y., He, C.Y., Ehrhardt, A., Kay, M.A., 2003. Minicircle DNA vectors devoid of bacterial DNA result in persistent and high-level transgene expression in vivo. Mol. Ther. 8, 495–500.

Chen, Z.Y., He, C.Y., Meuse, L., Kay, M.A., 2004. Silencing of episomal transgene expression by plasmid bacterial DNA elements, in vivo. Gene Ther. 11, 856–864.

Chen, K.T., Chang, H.L., Wang, S.T., Cheng, Y.T., Yang, J.Y., 2007. Epidemiologic features of hand–foot–mouth disease and herpangina caused by enterovirus 71 in Taiwan, 1998–2005. Pediatrics 120, 244–252.

Darquet, A.M., Cameron, B., Wils, P., Scherman, D., Crouzet, J., 1997. A new DNA vehicle for nonviral gene delivery: supercoiledminicircle. Gene Ther. 4, 1341–1349.

Darquet, A.M., Rangara, R., Kreiss, P., Schwartz, B., Naimi, S., Delaère, P., Crouzet, J., Scherman, D., 1999. Minicircle: an improved DNA molecule for in vitro and in vivo gene transfer. Gene Ther. 6, 209–218.

Fire, A., Xu, S., Montgomery, M.K., Kostas, S.A., Driver, S.E., Mello, C.C., 1998. Potent and specific genetic interference by double-stranded RNA in *Caenorhabditis elegans*. Nature 391, 806–811.

Gao, Y.Z., Sun, L., Dong, J., Xu, X.Y., Shu, Y.L., Chen, M.H., Yin, L., Liang, Z.C., Jin, Q., 2006. Rapid identification of small interfering RNA that can effectively inhibit the replication of multiple influenza B virus strains. Antivir. Ther. 11, 431–438.

Giladi, H., Ketzinel-Gilad, M., Rivkin, L., Felig, Y., Nussbaum, O., Galun, E., 2003. Small interfering RNA inhibits hepatitis B virus replication in mice. Mol. Ther. 8, 769–776.

Gilbert, G.L., Dickson, K.E., Waters, M.J., Kennett, M.L., Land, S.A., Sneddon, M., 1988. Outbreak of enterovirus 71 infection in Victoria, Australia, with a high incidence of neurologic involvement. Pediatr. Infect. Dis. J. 7, 484–488.

Gitlin, L., Karelsky, S., Andino, R., 2002. Short interfering RNA confers intracellular antiviral immunity in human cells. Nature 418, 430–434.

Haasnoot, J., Westerhout, E.M., Berkhout, B., 2007. RNA interference against viruses: strike and counterstrike. Nat. Biotechnol. 25, 1435–1443.

Ho, M., Chen, E.R., Hsu, K.H., Twu, S.J., Chen, K.T., Tsai, S.F., Wang, J.R., Shih, S.R., 1999. An epidemic of enterovirus 71 infection in Taiwan. Taiwan Enterovirus Epidemic Working Group. N. Engl. J. Med. 341, 929–935.

Ishimaru, Y., Nakano, S., Yamaoka, K., Takami, S., 1980. Outbreaks of hand, foot, and mouth disease by enterovirus 71. High incidence of complication disorders of central nervous system. Arch. Dis. Child. 55, 583–588.

Jacque, J.M., Triques, K., Stevenson, M., 2002. Modulation of HIV-1 replication by RNA interference. Nature 418, 435–438.

Jechlinger, W., 2006. Optimization and delivery of plasmid DNA for vaccination. Exp. Rev. Vaccin. 5, 803–825.

Li, Y., Wasser, S., Lim, S.G., Tan, T.M., 2004. Genome-wide expression profiling of RNA interference of hepatitis B virus gene expression and replication. Cell. Mol. Life Sci. 61, 2113–2124.

Liu, Y.P., Haasnoot, J., Berkhout, B., 2007. Design of extended short hairpin RNAs for HIV-1 inhibition. Nucleic Acids Res. 35, 5683–5693.

Lu, W.W., Hsu, Y.Y., Yang, J.Y., Kung, S.H., 2004. Selective inhibition of enterovirus 71 replication by short hairpin RNAs. Biochem. Biophys. Res. Commun. 325, 494–499.

Lyon, A.R., Sato, M., Hajjar, R.J., Samulski, R.J., Harding, S.E., 2008. Gene therapy: targeting the myocardium. Heart 94, 89–99.

Marshall, E., 1999. Gene therapy death prompts review of adenovirus vector. Science 286, 2244–2245.

Phipps, K.M., Martinez, A., Lu, J., Heinz, B.A., Zhao, G.S., 2004. Small interfering RNA molecules as potential anti-human rhinovirus agents: in vitro potency, specificity, and mechanism. Antiviral Res. 61, 49–55.

Qiu, J., 2008. Enterovirus 71 infection: a new threat to global public health? Lancet Neurol. 7, 868–869.

Racaniello, V.R., 2007. Picornaviridae: the viruses and their replication. In: Knipe, D.M. et al. (Eds.), Fields Virology, fifth ed. Lippincott Williams & Wilkins, Philadelphia, PA, pp. 796–839.

Robinson, C.R., Doane, F.W., Rhodes, A.J., 1958. Report of an outbreak of febrile illness with pharyngeal lesions and exanthem: Toronto, summer 1957: isolation of group A Coxsackie virus. Can. Med. Assoc. J. 79, 615–621.

Shinohara, M., Uchida, K., Shimada, S., Segawa, Y., Hoshino, Y., 2001. Characterization of enterovirus type 71 isolated in Saitama Prefecture in 2000. Kansenshogaku Zasshi 75, 490–494.

Sim, A.C., Luhur, A., Tan, T.M., Chow, V.T., Poh, C.L., 2005. RNA interference against enterovirus 71 infection. Virology 341, 72–79.

Solomon, T., Lewthwaite, P., Perera, D., Cardoso, M.J., McMinn, P., Ooi, M.H., 2010. Virology, epidemiology, pathogenesis, and control of enterovirus 71. Lancet Infect. Dis. 10, 778–790.

Tan, E.L., Tan, T.M.C., Chow, V.T.K., Poh, C.L., 2007. Enhanced potency and efficacy of 29-mer shRNAs in inhibition of Enterovirus 71. Antiviral Res. 74, 9–15.

Wang, C.Y., Li Lu, F., Wu, M.H., Lee, C.Y., Huang, L.M., 2004. Fatal coxsackievirus A16 infection. Pediatr. Infect. Dis. J. 23, 275–276.

Wong, K.T., Munisamy, B., Ong, K.C., Kojima, H., Noriyo, N., Chua, K.B., Ong, B.B., Nagashima, K., 2008. The distribution of inflammation and virus in human enterovirus 71 encephalomyelitis suggests possible viral spread by neural pathways. J. Neuropathol. Exp. Neurol. 67, 162–169.

Wright Jr., H.T., Landing, B.H., Lennette, E.H., Mcallister, R.M., 1963. Fatal infection in an infant associated with Coxsackie virus group A, type 16. N. Engl. J. Med. 268, 1041–1044.

Wu, Z.Q., Gao, Y.Z., Sun, L.L., Tien, P., Jin, Q., 2008. Quick identification of effective small interfering RNAs that inhibit the replication of coxsackievirus A16. Antiviral Res. 80, 295–301.

Wu, Z.Q., Yang, F., Zhao, R., Zhao, L.N., Guo, D.Y., Jin, Q., 2009. Identification of small interfering RNAs which inhibit the replication of several Enterovirus 71 strains in China. J. Virol. Methods 159, 233–238.

Yip, C.C., Lau, S.K., Zhou, B., Zhang, M.X., Tsoi, H.W., Chan, K.H., Chen, X.C., Woo, P.C., Yuen, K.Y., 2010. Emergence of enterovirus 71 "double-recombinant" strains belonging to a novel genotype D originating from southern China: first evidence for combination of intratypic and intertypic recombination events in EV 71. Arch. Virol. 155, 1413–1424.

Yokota, T., Sakamoto, N., Enomoto, N., Tanabe, Y., Miyagishi, M., Maekawa, S., Yi, L., Kurosaki, M., Taira, K., Watanabe, M., Mizusawa, H., 2003. Inhibition of intracellular hepatitis C virus replication by synthetic and vector-derived small interfering RNAs. EMBO Rep. 4, 602–608.

Yuan, J., Cheung, P.K., Zhang, H.M., Chau, D., Yang, D., 2005. Inhibition of coxsackievirus B3 replication by small interfering RNAs requires perfect sequence match in the central region of the viral positive strand. J. Virol. 79, 2151–2159.

Zhang, D., Lu, J., 2010. Enterovirus 71 vaccine: close but still far. Int. J. Infect. Dis. 14, 739–743.

Zhang, Y., Wang, D., Yan, D., Zhu, S., Liu, J., Wang, H., Zhao, S., Yu, D., Nan, L., An, J., Chen, L., An, H., Xu, A., Xu, W., 2010. Molecular evidence of persistent epidemic and evolution of subgenotype B1 coxsackievirus A16-associated hand, foot, and mouth disease in China. J. Clin. Microbiol. 48, 619–622.

Zhou, H., Jin, M., Yu, Z., Xu, X., Peng, Y., Wu, H., Liu, J., Liu, H., Cao, S., Chen, H., 2007. Effective small interfering RNAs targeting matrix and nucleocapsid protein gene inhibit influenza A virus replication in cells and mice. Antiviral Res. 76, 186–193.